PHYSICAL REVIEW B VOLUME 17, NUMBER 3 1 FEBRUARY 1978

Composite solitons and magnetic resonance in superfluid ^{3}He-A. II*

Kazumi Maki and Pradeep Kumar
Physics Department, University of Southern California, Los Angeles, California 90007
(Received 20 May 1977; revised manuscript received 8 August 1977)

A recent study on composite solitons in ^{3}He-A is extended to more general configurations and to all temperatures. The texture free energy and the NMR satellite frequencies are determined. In particular, the satellite frequency associated with the splay composite soliton appears to account for the transverse satellite observed by Gould and Lee.

I. INTRODUCTION

In recent papers[1,2] we have shown that among planar structures in ^{3}He-A a twistlike composite soliton has the lowest energy. In the composite soliton both the $\hat{l}$ (designating the symmetry axis of the quasiparticle energy gap) and the $\hat{d}$ (describing the spin component of the condensate) vectors rotate within the same plane but in the opposite direction. In an open system this composite soliton has also been shown to be the end product of the decay of a pure $\hat{d}$ soliton. We have further calculated the satellite NMR frequencies in the presence of the twist composite soliton and found excellent agreement with that observed in the longitudinal experiments by the Orsay-Saclay group[3] and by Gould and Lee.[4] On the other hand, the predicted transverse satellite frequency was a little larger than that observed by Gould and Lee.[4] We suggested that the transverse satellite may arise from a related but different texture. In fact, we will show that the experimental procedure used to observe the transverse satellite by Gould and Lee[4] produces the splay composite soliton. Furthermore, the corresponding transverse satellite frequency accounts beautifully for the observed transverse satellite.

The object of this paper is to consider the other possible composite solitons and study their NMR response. We have noted earlier the three typical planar textures[5]; splay, bending, and twist. The twist structure has already been studied in Ref. 2. This classification is based on the relative orientation of $\hat{k}$, the unit vector normal to the domain wall, and $\hat{l}_0$ (or $\hat{d}_0$) the asymptotic orientation of $\hat{l}$ (or $\hat{d}$). In a (long) cylinder for example the lowest-energy texture would require $\hat{k}$ to be parallel to the cylindrical axis, since in this configuration the surface area associated with the planar texture is minimized. More generally in any container with two open ends, the most favorable textures appear to be those with the domain walls parallel to the end surfaces. $\hat{k}$ is furthermore the direction of the space inhomogeneity, which is assumed fixed in the following analysis. In the presence of a static magnetic field $\vec{H}_0$, we can further assume that $\hat{l}$ and $\hat{d}$ lie in a plane perpendicular to $\vec{H}_0$. Therefore, in a long cylinder, the direction of the static magnetic field determines uniquely the texture involved. In particular, when $\vec{H}_0$ is parallel to the cylindrical axis as in the longitudinal experiment by Gould and Lee, we have the pure twist texture. On the other hand, in their transverse experiment $\vec{H}_0$ was applied perpendicular to the cylindrical axis. In this situation we cannot have the twist texture but the splay-bending texture. (We shall call hereafter the splay-bending composite soliton with the lowest energy simply the splay composite soliton.) More generally, if $\vec{H}_0$ makes an angle θ to $\hat{k}$, the relevant texture changes continuously from the pure twist texture for $\theta = 0$ to the splay texture for $\theta = \pi/2$ as θ increases from 0 to $\pi/2$. We predict that, if the experiment is done with a static magnetic field $\vec{H}_0$ with an angle θ to the axis of the cylinder, one can see a continuous change of the texture involved in the form of continuous changes in satellite frequencies from the pure twist case to the splay case. An obvious advantage in this setup is that one can pick up both the longitudinal and the transverse signal simultaneously with a single rf field along the cylindrical axis.

Another particular feature of the Cornell satellites[4] is their temperature dependence. The longitudinal satellite frequency normalized by the Leggett frequency has been found to be weakly temperature dependent, whereas the transverse one is almost insensitive to temperature. We have suggested earlier that this temperature dependence can be understood in terms of the temperature-dependent Fermi-liquid corrections to the Ginzburg-Landau free energy as proposed by Cross.[6] Basically the coefficients in the texture free energy are expressed in terms of the superfluid densities (mass as well as spin) which have different temperature dependence. This results in temperature-dependent satellite frequencies. We find that the transverse satellite frequency is in general

less sensitive to temperature variations than the longitudinal satellite frequency.

The calculations for the temperature dependence will be reported both for the splay composite as well as twist composite solitons. For the twist composite soliton, the temperature dependence can be obtained exactly in terms of a parameter κ_7 (to be defined later in Sec. IV) which depends on the spin and the mass superfluid density and the Fermi-liquid parameters. For the splay composite soliton the result is given only for T near T_c. Comparison of our results with the observed temperature dependence of satellite frequencies yield a value for F_1^a (= −1.02 at the melting pressure) quite similar to values estimated earlier.[7,8]

In Sec. II, we first calculate the free energy and the profile associated with the composite soliton, where the space gradients (direction of $\hat{k}$) makes an arbitrary angle θ to H_0 ($0<\theta<\pi/2$). In Sec. III, we present the calculation of satellite frequencies for the longitudinal as well as transverse magnetic resonance. Section IV includes generalization of the texture free energy for all temperatures and a discussion of temperature dependence of satellite frequencies due to the temperature-dependent Fermi-liquid corrections. Section V includes a summary of results. In the Appendix, we present the results for bending structure.

In all of the calculations reported here, the A-phase order parameter is given by $A_{\mu i}=d_\mu\Delta_i$, with

$$\Delta_i=(\Delta_0/\sqrt{2})e^{i\Phi}(\hat{\delta}_1+i\hat{\delta}_2)_i\,, \tag{1}$$

where $\hat{\delta}_1$, $\hat{\delta}_2$, and $\hat{l}$ ($\equiv\hat{\delta}_1\times\hat{\delta}_2$) constitute an orthogonal triad of unit vectors describing the orbital component and $\hat{d}$ represents a unit vector describing the spin component of the order parameter. The spatial variation of these vectors is determined in the Ginzburg-Landau regime[9] by the free energy $F=F_{\rm kin}+E_D$, where

$$F_{\rm kin}=\frac{1}{2}K\int d^3r\,[3|\vec{\nabla}\cdot\vec{\Delta}|^2+|\vec{\nabla}\times\vec{\Delta}|^2+2|(\vec{\Delta}\cdot\vec{\nabla})\hat{d}|^2 + |\vec{\Delta}|^2(|\vec{\nabla}\cdot\hat{d}|^2+|\vec{\nabla}\times\hat{d}|^2)]\,, \tag{2}$$

where in the weak coupling theory K is given by[10]

$$K=\frac{6}{5}\frac{N}{(8m^*)}\frac{7\zeta(3)}{(2\pi T_c)^2}\,.$$

In the presence of a strong magnetic field $\vec{H}_0$ in the z direction, both $\hat{d}$ and $\hat{l}$ are constrained in the x-y plane;

$$\hat{d}=\sin\psi\hat{x}+\cos\psi\hat{y}\,,$$

$$\hat{l}=\sin\chi\hat{x}+\cos\chi\,\hat{y}\,,$$

and

$$\vec{\Delta}=\frac{\Delta_0}{\sqrt{2}}e^{-\Phi}(-\cos\chi\hat{x}+\sin\chi\,\hat{y}+i\hat{z})\,. \tag{3}$$

For planar textures Eq. (2) can be processed with the assumption that Φ, χ, and ψ depend only on $s=\hat{k}\cdot\vec{x}$, where $\vec{k}$ is a unit vector normal to the domain wall.

This has already been done in detail in Ref. 2. Minimizing the free energy $F_{\rm kin}$ in terms of Φ, we can express Φ_s in terms of χ_s. Then eliminating Φ_s we have

$$f=\frac{F}{\sigma(\hat{k})}=\frac{1}{2}A\int ds\Big[\Big(1+2a^2-\frac{2k_3^2a^2}{2-a^2}\Big)\chi_s^2 + 2(2-a^2)\psi_s^2+\frac{4}{\xi_1^2}\sin^2(\chi-\psi)\Big]\,. \tag{4}$$

Here $A=\frac{1}{2}K\Delta_0^2=\frac{1}{4}\chi_N C^2$, where C is the spin-wave velocity with the propgation vector perpendicular to $\hat{l}$, $a=k_1\sin\chi+k_2\cos\chi$ with $\hat{k}=(k_1,\ k_2,\ k_3)$ and $\xi=C/\Omega_A$, is the dipolar-coherence length. Ω_A is the longitudinal NMR frequency in ^{3}He-A, $\sigma(\hat{k})$ is the surface area of the domain wall. In Eq. (4) we include the dipolar interaction energy E_D (the last term). We also have

$$\Phi_s=k_3a\chi_s/(2-a^2)\,. \tag{5}$$

The phase current is thus nonvanishing only if $k_3k_\perp=0$ with $k=(k_1^2+k_2^2)^{1/2}$. Therefore, in the limits $\vec{H}_0\|\hat{k}$ and $\vec{H}_0\perp\hat{k}$, the phase current vanishes identically.

II. TEXTURE ENERGY AND PROFILE

We study the case when $\hat{k}=(0,\ \sin\theta,\ \cos\theta)$ the vector normal to the domain wall makes an angle θ with respect to the direction of the static magnetic field. For $\theta\neq0$, the free energy [Eq. (4)] is nonseparable and we resort to two approximations. In the first approximation, recalling that the principal independent variable in the twist composite soliton was the relative angle $v=\chi-\psi$, we express the free energy in terms of v and $\chi=\alpha v+c$, where α is a variational parameter and c, (a constant) is fixed by the orientation of the vector in the middle of the domain wall. If $\chi=\frac{1}{2}\pi$ at the center ($v=\frac{1}{2}\pi$) we have $c=(1-\alpha)\frac{1}{2}\pi$ and the structure obtained has a splay conformation for the $\hat{l}$ vector but a bend conformation for the $\hat{d}$ vector. This texture is the same as the case $\theta=\frac{1}{2}\pi$ analyzed below. If $\chi=0$ at the center, $c=-\alpha\frac{1}{2}\pi$, the texture obtained is bend-like for $\hat{l}$, and is discussed in Appendix A.

For the second approximation, we assume $\sin v=\mathrm{sech}(\eta s)$. Again η which represents the width of the domain wall is treated as a variational parameter. The approximation is necessary in order to calculate the resonance frequencies [see Sec. III]. A numerical calculation has been done without the last approximation to test its validity and is reported in Appendix B.

TABLE I. Results for the arbitrary angle field.

			Long.		Trans.	
θ	α	f_θ^c/f^d	R_l	ν	R_t	μ
90.0	0.6981	0.495	0.635	0.415	0.823	0.309
82.3	0.7	0.494	0.637	0.413	0.825	0.307
70.3	0.71	0.489	0.646	0.402	0.832	0.296
62.9	0.72	0.484	0.655	0.392	0.840	0.285
56.7	0.73	0.479	0.664	0.382	0.847	0.274
51.1	0.74	0.474	0.673	0.371	0.854	0.263
45.7	0.75	0.470	0.682	0.361	0.861	0.253
40.3	0.76	0.465	0.691	0.350	0.868	0.242
34.6	0.77	0.460	0.700	0.340	0.875	0.232
28.1	0.78	0.456	0.709	0.329	0.881	0.221
19.9	0.79	0.451	0.719	0.318	0.889	0.211
0.0	0.80	0.447	0.729	0.306	0.894	0.200

A straightforward calculation following Eq. (4) yields

$$f_\theta^c = (\eta\xi_\perp)^{-1} f^d , \tag{6}$$

where

$$4(\eta\xi_\perp)^{-2} \cong \alpha^2 + 4(\alpha-1)^2 + \tfrac{2}{3}\alpha^2 \sin^2\theta \times (2\alpha - 1 - \tfrac{1}{2}\alpha^2\cos^2\theta) , \tag{7}$$

where $f^d = 8A\xi_\perp^{-1}$ is the surface energy of a twist d soliton. In deriving Eq. (7), we have first integrated the integrand over s, by expanding the integrand in powers of α and retaining the terms up to the order of α^4. Then we have minimized the expression in terms of η. The free energy f_θ^c is then obtained by minimizing $(\eta\xi)^{-1}$ separately for each angle θ by varying α and the results along with the satellite resonance frequencies are summarized in Table I. One of our approximations (i.e., the expansion in power of α) is justified *a posteriori*, since $\alpha^2 \leq 0.64$. In particular, for $\theta = 0$ (the pure twist case) the variational function to the exact solution already found in I. For $\theta = \frac{1}{2}\pi$, the composite soliton consists of splaylike $\hat{l}$ texture and bendlike $\hat{d}$ texture. See Figs. 1 and 2 for the definition of twist, splay, and bend. The calculation of resonance frequencies is described in Sec. III.

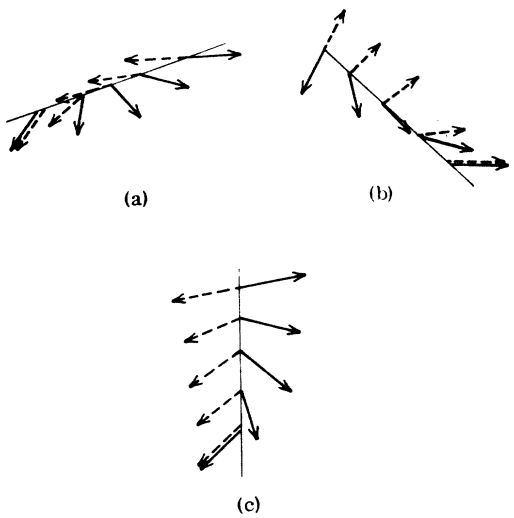

FIG. 1. Three possible conformations for a composite soliton: (a) a splay structure, (b) a bending structure, and (c) a twist structure. The solid arrows are the directions of the $\hat{l}$ vector, the dotted arrows represent the $\hat{d}$ vectors.

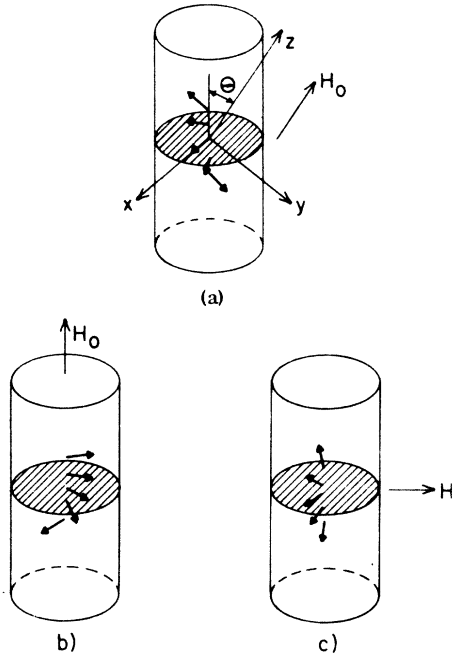

FIG. 2. Textures in a cylinder in the presence of magnetic field. Only the $\hat{l}$ vectors are shown: (a) Shows the static field $\vec{H}_0$ at an angle θ with respect to the cylinder axis. (b) and (c) show the twist and splay composite with the field, respectively, parallel and perpendicular to the cylinder axis.

III. MAGNETIC RESONANCES

We have already discussed the possibility of a localized mode of oscillation of the $\hat{d}$ vector. This mode can be magnetically excited and may be responsible for the satellite observed in the longitudinal or transverse resonance. In order to calculate the resonance frequencies we begin with the $\hat{d}$ vector given by

$$\hat{d} = \cos g\,[\sin(\psi_0 + f)\,\hat{x} + \cos(\psi_0 + f)\,\hat{y}] + \sin g\,\hat{z} , \tag{8}$$

where ψ_0 describes the equilibrium $\hat{d}$ configuration in the presence of a composite soliton, and f and

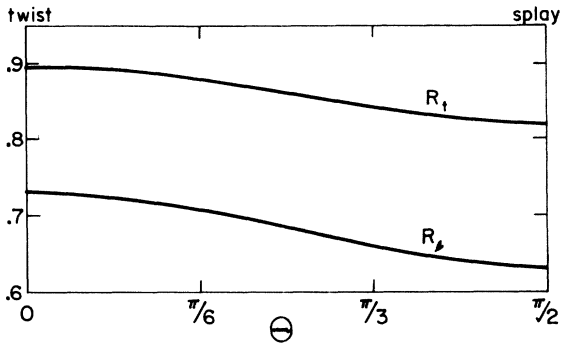

FIG. 3. θ dependence of the ratios for the longitudinal R_l and transverse R_t satellite frequencies. The texture at $\theta=0$ is a twist composite, while the one at $\theta=\pi/2$ is a splay composite soliton.

g describe small fluctuations of $\hat{d}$ around the equilibrium configuration. The spin-fluctuation free energy is then obtained by substituting Eq. (8) into Eq. (4) and expanding in powers of f and g. Retaining the terms quadratic in f and g we have when $\hat{k}$ makes an angle θ to $\vec{H}_0$,

$$\delta f = 2A \int ds\, [(1-\tfrac{1}{2}\sin^2\theta\cos^2\chi_0)(f_s^2+g_s^2) + \xi_1^{-2}((1-2\sin^2 v_0)f^2+\{1-[1+(\alpha-1)^2(\eta\xi_1)^2 \times(1-\tfrac{1}{2}\sin^2\theta\cos^2\chi_0)]\sin^2 v\}g^2)], \quad (9)$$

where χ_0 and v_0 are corresponding variables describing the equilibrium configuration. As to the equilibrium configuration we have made use of a solution determined variationally in Sec. II; for example, $\chi_0 \cong \alpha \cos v_0 = \alpha \tanh(\eta s)$, and both α and η are functions of angle θ as given in Table I.

Equation (9) is recast into the eigenvalue equations

$$\lambda_f f = \Lambda_f f = -\frac{1}{2}\xi_1^2 \frac{d}{dy}[(1+\sin^2\chi_0)f_y] + (1-2\sin^2 v_0)f, \quad (10a)$$

and

$$\lambda_g g = \Lambda_g g = -\frac{1}{2}\xi_1^2 \frac{d}{dy}[(1+\sin^2\chi_0)g_y] + \left\{1-\left[1+\frac{1}{2}(\alpha-1)^2(\eta\xi_1)^2 \times(1+\sin^2\chi_0)\right]\sin^2 v_0\right\} g. \quad (10b)$$

The corresponding eigenvalue equations are solved variationally for each angle assuming that $f \propto (\mathrm{sech}\eta s)^\nu$ and $g \propto (\mathrm{sech}\eta s)^\mu$. The results are given in Table I. The parameters $R_l(\equiv \lambda_f^{1/2})$ and $R_t(\equiv \lambda_g^{1/2})$ which appears in the satellite frequency[2] as

$$\omega_l = R_l \Omega_A$$
$$(\omega_t^2 - \omega_0^2)^{1/2} = R_t \Omega_A \quad (11)$$

are also shown as function of θ in Fig. 3. Here ω_l and ω_t are the longitudinal and the transverse satellite, respectively. From Fig. 3 we see that both R_l and R_t decrease continuously from the values corresponding to the pure twist composite soliton to those of the splay soliton as θ increases from 0 to $\frac{1}{2}\pi$.

Of particular interest is the case $\theta=\frac{1}{2}\pi$ (i.e., the splay composite soliton), where we have

$$R_l = 0.635 \quad \text{and} \quad R_t = 0.823 \quad (12)$$

for the longitudinal and transverse resonance, respectively. We believe that the splay composite soliton is responsible for the transverse satellite frequency in the Gould-Lee (GL) experiment.[4] This identification is based on not only that the present satellite frequency is in excellent agreement with the observed value, but also that it is the unique stable texture when the static magnetic field is perpendicular to the axis of the cylinder as in their experiment.

IV. BEYOND THE GL REGIME

The frequency ratios R_l and R_t within the weak coupling theory are pure numbers independent of pressure and/or temperature (at least in the GL regime). However, at lower temperatures they do acquire the temperature dependence due to the temperature dependence of the Fermi-lquid corrections as discussed by Cross.[6] Cross has noted that near T_c the effect of Fermi-liquid corrections is to simply replace m by m^*. This has no effect on the above frequency ratios. Below T_c, however, the spin and the mass superfluid currents acquire different Fermi-liquid corrections, resulting in an additional temperature dependence on R_l and R_t.

According to Cross[6] the generalized free energy is given by

$$F_{\mathrm{kin}} = \tfrac{1}{2}\chi_N C_\perp^2 \int d^3r \{\kappa_1(\hat{l}\cdot\vec{\nabla}\Phi)^2 + \kappa_2(\hat{l}\times\vec{\nabla}\Phi)^2 + \kappa_3(\vec{\nabla}\Phi)\cdot[\mathrm{curl}\,\hat{l} - \hat{l}(\hat{l}\cdot\mathrm{curl}\,\hat{l})] - \kappa_4(\vec{\nabla}\Phi)\cdot\hat{l}(\hat{l}\,\mathrm{curl}\,\hat{l}) + \kappa_5(\mathrm{div}\hat{l})^2 + \kappa_6(\hat{l}\times\mathrm{curl}\,\hat{l})^2 + \kappa_7(\hat{l}\cdot\mathrm{curl}\,\hat{l})^2 + |(\hat{l}\times\vec{\nabla})\hat{d}|^2 + \lambda|(\hat{l}\cdot\vec{\nabla})\hat{d}|^2\}, \quad (13)$$

where

$$\kappa_1=\rho_{s\parallel}/\rho_{s\perp}^{\rm spin},\quad \kappa_2=\rho_{s\perp}/\rho_{s\perp}^{\rm spin},\quad \kappa_3=\kappa_2(\rho_{s\parallel}^0/\rho_{s\perp}^0),\quad \kappa_4=\kappa_1,\quad \kappa_5=\tfrac{1}{4}(1+\tfrac{1}{3}F_1)^{-1}\rho_{s\perp}^0/\rho_{s\perp}^{\rm spin},$$
$$\kappa_6=(1+\tfrac{1}{3}F_1)^{-1}\left(\frac{1}{2}\rho_{s\parallel}^0+\frac{1}{12}\frac{F_1}{1+\frac{1}{3}F_1(\rho_{n\perp}^0/\rho)}\rho_{s\parallel}^0\frac{\rho_{s\parallel}^0}{\rho}+\tfrac{2}{3}\tilde{\gamma}\rho\right)/\rho_{s\perp}^{\rm spin},\tag{14}$$
$$\kappa_7=\tfrac{1}{3}(1+\tfrac{1}{3}F_1)^{-1}\left(\frac{1}{4}\rho_{s\perp}^0+\rho_{s\parallel}^0+\frac{1}{4}\frac{F_1}{1+\frac{1}{3}F_1(\rho_{n\parallel}^0/\rho)}\rho_{s\parallel}^0(\rho_{s\parallel}^0/\rho)\right)/\rho_{s\perp}^{\rm spin},$$
$$\lambda=\rho_{s\parallel}^{\rm spin}/\rho_{s\perp}^{\rm spin},\quad \chi_N C_\perp^2=(\hbar^2/2m)^2\rho_{s\perp}^{\rm spin},$$

and ρ_{si}, $\rho_{si}^{\rm spin}$, and ρ_{si}^0 are the mass, the spin, and the irreducible superfluid density, and γ is another quantity introduced by Cross,

$$\tilde{\gamma}=3\int\frac{d\Omega}{4\pi}\frac{\hat{p}_3^4}{1-\hat{p}_3^2}\phi(\hat{p})$$

and

$$\phi(\hat{p})=1-\frac{\beta}{2}\int_0^\infty d\epsilon\,{\rm sech}^2\tfrac{1}{2}\beta E(\hat{p})$$

with

$$E(\hat{p})=\epsilon^2+\Delta^2(1-\hat{p}_3^2)^{1/2}.\tag{15}$$

Here we have written $F_{\rm kin}$ in terms of $\hat{l}$ and Φ rather than in $\hat{\Delta}=\sqrt{2}\vec{\Delta}/\Delta_0$, which is more convenient in this general circumstance. Furthermore χ_N is the normal state-spin susceptibility and $C_\perp$ is the spin-wave velocity with the propagation vector perpendicular to $\hat{l}$. Now the temperature-dependent Fermi-liquid corrections are easily incorporated into Eq. (13), making use of the relation due to Leggett[11]

$$\rho_{s\perp,\parallel}=(1-\phi_{\perp,\parallel})/(1+\tfrac{1}{3}F_1\phi_{\perp,\parallel})$$

and

$$\rho_{s\perp,\parallel}^{\rm spin}=(1+\tfrac{1}{3}F_1^a)/(1+\tfrac{1}{3}F_1)\cdot(1-\phi_{\perp,\parallel})/(1+\tfrac{1}{3}F_1^a\phi_{\perp,\parallel}),$$

with $\phi_{\perp,\parallel}=\rho_{s\perp,\parallel}^0/\rho$, where F_1 and F_1^a are the P-wave Landau coefficients.

In particular, within the weak-coupling model the above coefficients are given by

$$\kappa_1=\kappa_4=\tfrac{1}{2}+\tfrac{1}{3}(\tfrac{1}{2}A_1-B_1)\epsilon,\quad \kappa_2=1+\tfrac{2}{3}(A_1-B_1)\epsilon,$$
$$\kappa_3=\tfrac{1}{2}+\tfrac{1}{3}(A_1-B_1)\epsilon,\quad \kappa_5=\tfrac{1}{4}-\tfrac{1}{6}B_1\epsilon,$$
$$\kappa_6=\tfrac{3}{4}+\tfrac{1}{2}(\tfrac{1}{3}A_1-B_1)\epsilon,\quad \kappa_7=\tfrac{1}{4}+\tfrac{1}{6}(\tfrac{1}{4}A_1-B_1)\epsilon,$$

and

$$\lambda=\tfrac{1}{2}-\tfrac{1}{6}B_1\epsilon\quad\text{for}\quad T\cong T_c,\tag{16}$$

with

$$\epsilon=(T_c-T)/T_c,\quad A_1=F_1/(1+\tfrac{1}{3}F_1),$$

and

$$B_1=F_1^a/(1+\tfrac{1}{3}F_1^a),$$

and

$$\kappa_1=\kappa_2=\kappa_3=\kappa_4=(3+F_1)/(3+F_1^a),\quad \kappa_5=\tfrac{1}{4}(1+\tfrac{1}{3}F_1^a)^{-1},$$
$$\kappa_6=\kappa_5[2+\tfrac{1}{3}F_1+8\ln(2\gamma\Delta/\pi T)-\tfrac{32}{3}],\tag{17}$$
$$\kappa_7=\tfrac{1}{3}\kappa_5(5+F_1),\quad \lambda=1$$

for $T\cong 0$ where $\gamma=1.76$ is the Euler constant.

We note first that the anistropy in ρ_{si} and $\rho_{si}^{\rm spin}$ disappear completely at $T=0$ K. On the other hand, κ_6 diverges logarithmically as T approaches O. Since any composite soliton except the pure twist soliton involves the term with κ_6 coefficient, these solitons become pure $\hat{d}$ solitons as the temperature is lowered. However, even in the case of the pure twist composite soliton, it becomes very close to the $\hat{d}$ soliton since $\kappa_i\gg 1$ for $T\cong 0$.

We shall first consider the twist composite soliton, which can be solved exactly at all temperatures. Assuming that $\hat{d}$, $\hat{l}$, and $\vec{\Delta}$ are given by Eq. (3) and that $\hat{k}=\hat{z}$, Eq. (13) is reduced to

$$f_{\rm twist}^c=\frac{F}{\sigma(\hat{z})}=\frac{1}{8}\chi_N C_\perp^2\int dz\,[\psi_z^2+\kappa_7\chi_z^2+\xi_\perp^{-2}\sin^2(\chi-\psi)].\tag{18}$$

We note here that the composite soliton depends only on κ_7. Introducing new variables by

$$U=\psi+\kappa_7\chi,\quad v=\chi-\psi.\tag{19}$$

Equation (18) is reduced to

$$f_{\rm twist}^c=\frac{1}{8}\chi_N C^2\int dz\left(\frac{U_z^2}{1+\kappa_7}+\frac{\kappa_7}{1+\kappa_7}v_z^2+\xi_\perp^{-2}\sin^2 v\right),\tag{20}$$

which has a soliton solution with $U=$ const and

$$\tan v/2=\exp[(\kappa_7^{-1}+1)^{1/2}z/\xi_\perp].\tag{21}$$

This solution yields

$$f_{\rm twist}^c=(1+\kappa_7^{-1})^{-1/2}f^d$$

and

$$f^d=\chi_N C_\perp^2\xi_\perp^{-1}.\tag{22}$$

The spin fluctuation around the composite soliton can be treated similarly and we have

$$R_l=\tfrac{1}{2}[((\kappa_7^{-1}+1)(\kappa_7^{-1}+9))^{1/2}-(\kappa_7^{-1}+3)]^{1/2}$$

and

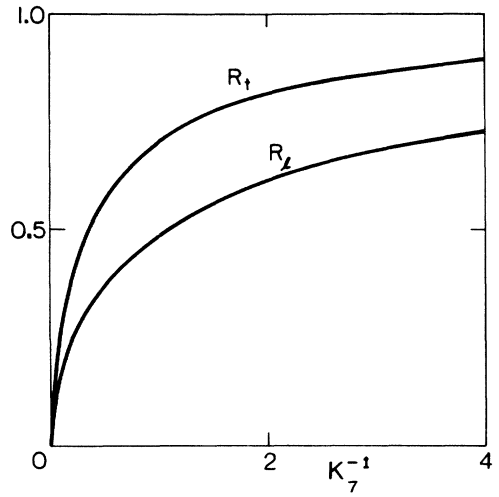

FIG. 4. Temperature dependence of R_l and R_t for a twist composite shown here in terms of dependence on the parameter κ_7^{-1} defined in Eq. (15). At the melting pressure κ_7^{-1} varies from 4 at $T=T_c$ to around 0.1 at $T=0$.

$$R_t=[\kappa_7^{-1}/(1+\kappa_7^{-1})]^{1/2} \tag{23}$$

for the ratios in the longitudinal and the transverse satellite frequencies. The above ratios R_l and R_t are shown as functions of κ_7^{-1} in Fig. 4. Since κ_7 increases as the temperature decreases below T_c, R_l and R_t decrease monotonically as the temperature decreases. Substituting κ_7 given in Eq. (16) and expanding in ϵ, we can estimate the temperature dependence of R_l and R_t for the twist soliton in the vicinity of T_c

$$R_l\cong 0.729-(0.027A_1-0.11B_1)\epsilon$$

and

$$R_t\cong 0.894-(0.015A_1-0.06B_1)\epsilon\,. \tag{24}$$

Now let us consider the case of the splay composite soliton. In this case the solution can be determined only approximately. In particular, variational parameters have to be determined at each temperature separately. However, if we limit ourselves in the vicinity of T_c, we can determine coefficients of ϵ in R_l and R_t by perturbation, by making use of the already known solution in the GL regime. This procedure yields, after a long but straightforward calculation

$$\begin{aligned} R_l&=0.635-(0.0003A_1-0.07B_1)\epsilon\,,\\ R_t&=0.823-(0.00015A_1-0.009B_1)\epsilon\,. \end{aligned} \tag{25}$$

Then, if we take our identification that the longitudinal satellite of the GL experiment is due to the twist composite soliton, while the transverse satellite is due to the splay soliton, we should have

$$(0.027A_1-0.11B_1)\cong 0.35 \tag{26a}$$

and

$$(0.00015A_1-0.009B_1)\cong 0\,, \tag{26b}$$

which follows from the use of the GL data $R_l=0.74-0.35\epsilon$ and $R_t\cong 0.835$. Since $F_1=15.66$ at the melting pressure, we can deduce F_1^a from Eq. (26a), we have $F_1^a=-1.33$. Substituting this in the left-hand side of Eq. (26b), we have

$$(0.00015A_1-0.009B_1)\cong 0.02\,,$$

which is appreciable but not inconsistent with the experimental data. We note that the above F_1^a value is very close to that obtained by Osheroff *et al.*[8] by analyzing the spin-wave velocity in ^{3}He-B within the weak-coupling theory.

The above weak-coupling analysis may be too simple for ^{3}He-A, as the axial phase is unstable in this limit. An approximate[12] way to incorporate the strong-coupling effect is to assume that the most important strong-coupling correction is in the normalization of $\Delta_0(T)^2$. (This we may call the naive strong-coupling theory.) This effect can be incorporated in our analysis by replacing ϵ in Eqs. (24) and (25) by $\epsilon^*\equiv[(\Delta C/C)\exp/(\Delta C/C)\text{weak}]\epsilon=1.5\epsilon$ at the melting pressure, where ΔC is the jump in the specific heat at T_c. Then comparing the predicted temperature dependence of R_l for the twist composite soliton with the experimental data, we have now $F_1^a=-1.01$, which is rather close to the value deduced by Wheatley[7] ($F_1^a=-0.55$) with the assumption $F_l=F_l^a=0$ for $l\geq 2$. More generally, from the position of the satellite resonance we can extract $\rho_{s\perp}^{\text{spin}}$ and $\rho_{s\parallel}^{\text{spin}}$ experimentally, if the temperature dependence of the superfluid density $\rho_{s\perp}$ and $\rho_{s\parallel}$ are known.

V. CONCLUDING REMARKS

We have extended previous study of composite solitons into two directions. First we have studied variationally a class of new textures which appear in the presence of a tilted magnetic field with respect to the normal vector of the domain wall. In particular, we identify two composite solitons, which are responsible for the longitudinal and the transverse satellites in ^{3}He-A. Furthermore, we propose an experimental setup, which enables one to explore a class of composite solitons. The corresponding satellite frequencies are obtained.

Secondly we generalize the texture free energy following the suggestion by Cross, which enables us to consider composite solitons at arbitrary temperatures. In particular, the temperature dependence of the observed ratio R_l and R_t are interpreted in terms of the temperature-dependent Fermi-liquid correction. This interpretation yields

an estimate of F_1^a, which is consistent with values deduced previously.

APPENDIX A

In Sec. II, the case with $C = -\alpha \frac{1}{2}\pi$ has been mentioned. In this case, the $\hat{l}$ vector bends while the $\hat{d}$ vector splays. Substituting the functions χ and v in Eq. (4), we obtain (we consider only $\theta = \pi/2$)

$$f^c_{\text{bending}} = (\zeta \xi_\perp)^{-1} f^d ,$$
$$4(\zeta \xi_\perp)^{-2} = \alpha^2 + 4(\alpha - 1)^2 + 2(2\alpha - 1)[1 - \tfrac{1}{3}\alpha^2] . \tag{A1}$$

After minimization this yields

$$\alpha = 0.413$$

and

$$(\zeta \xi_\perp)^{-1} = 0.5524 . \tag{A2}$$

The energy is larger than the splay case.

APPENDIX B

We now analyze the validity of the second approximation $\sin v = \operatorname{sech} \eta s$. With $\chi = \alpha v + c$; the splay profile $[c = (1 - \alpha)\frac{1}{2}\pi]$ is the solution of $\theta = \frac{1}{2}\pi$

$$v_y^2 = 4 \sin^2 v / [\xi_1^2 F(\alpha, v)] ,$$
$$F(\alpha, v) = \alpha^2 + 4(\alpha - 1)^2 + 2(2\alpha - 1)\cos^2 \chi . \tag{B3}$$

The energy is found to be the integral

$$f^c_{\text{splay}} = 2A \xi_1^{-1} \int_0^\pi dv \sin v [F(\alpha, v)]^{1/2} , \tag{B4}$$

which can be evaluated numerically and found to be $f^c_{\text{splay}} = 0.499 f^d$ ($\alpha = 0.695$); the agreement with Eq. (7) is excellent.

---

*Work supported by the NSF under Grant No. DMR76-21032.

[1]K. Maki and P. Kumar, Phys. Rev. Lett. 38, 557 (1977).
[2]K. Maki and P. Kumar, Phys. Rev. B 16, 182 (1977).
[3]O. Avenal, M. E. Bernier, E. J. Varoquaux, and C. Vibet, in *Proceedings of the XIV International Conference on Low Temperature Physics, Otaniemi, Finland, 1975*, edited by M. Krusius and M. Vuorio (North-Holland, Amsterdam, 1975), Vol. 5, p. 429.
[4]C. M. Gould and D. M. Lee, Phys. Rev. Lett. 37, 1223 (1976).
[5]K. Maki and P. Kumar, Phys. Rev. B 16, 174 (1977).
[6]M. C. Cross, J. Low Temp. Phys. 21, 525 (1975).
[7]J. C. Wheatley, *The Helium Liquid*, edited by J. G. M. Armytage and J. E. Farquhar (Academic, New York, 1975).
[8]D. D. Osheroff, W. Van Roosbroeck, H. Smith, and W. F. Brinkman, Phys. Rev. Lett. 38, 134 (1977).
[9]P. G. de Gennes, Phys. Lett. A 44, 271 (1973).
[10]V. Ambegaokar, P. G. de Gennes, and D. Rainer, Phys. Rev. A 9, 2676 (1974).
[11]A. J. Leggett, Phys. Rev. 140, A1869 (1965); also see Ref. 6, and R. Combescot, Phys. Rev. A 10, 1700 (1974).
[12]R. Combescot, Phys. Rev. Lett. 34, 8 (1975).